The Astrophysical Journal, 701:464–470, 2009 August 10 doi:10.1088/0004-637X/701/1/464

FORMATION OF COMPACT AMORPHOUS H_2O ICE BY CODEPOSITION OF HYDROGEN ATOMS WITH OXYGEN MOLECULES ON GRAIN SURFACES

Y. Oba[1], N. Miyauchi, H. Hidaka, T. Chigai, N. Watanabe, and A. Kouchi
Institute of Low Temperature Science, Hokkaido University, Sapporo, Hokkaido 060-0819, Japan; oba@lowtem.hokudai.ac.jp
Received 16 April 2009; accepted 5 June 2009; published 2009 July 23

ABSTRACT

Formation of H_2O molecules through the codeposition of oxygen molecules and hydrogen atoms is examined in situ using IR spectroscopy at 10–40 K under various O_2 and H fluxes. It is found that H_2O and H_2O_2 are continuously formed by reaction, even at 40 K. The H_2O ice formed is amorphous, but has a compact (not microporous) structure compared to vapor-deposited amorphous H_2O ice, because dangling OH bonds are not observed in the IR spectrum. This is consistent with astronomical observations in molecular clouds and theoretical predictions, which suggest that hydrogenation of O_2 is one of the potential routes for reproducing these IR spectral characteristics. The composition of the ice formed by codeposition varies with the O_2/H ratio and temperature. Although no data are available at present for the H_2O/H_2O_2 ratio of ice in molecular clouds, this study suggests that hydrogenation of O_2 has a potential to yield a H_2O/H_2O_2 ratio of 5 or more in molecular clouds.

Key words: atomic processes – ISM: clouds

1. INTRODUCTION

Interstellar icy grain mantles consist of various molecules such as H_2O, CO, CO_2, H_2CO, CH_3OH, and NH_3. Among these components, H_2O is predominant in dense molecular clouds (e.g., Gibb et al. 2004). The elucidation of H_2O formation in space is one of the most challenging objectives because of the ubiquity of H_2O in space and its significant importance for chemical evolution and the origin of life. Theoretical studies predict that the formation of H_2O in the gas phase is difficult to explain given the observed abundance in molecular clouds; therefore, it has been suggested that grain surface reactions are essential for the formation of H_2O in such environments (d'Hendecourt et al. 1985; Hasegawa et al. 1992; Hasegawa & Herbst 1993; Cuppen & Herbst 2007).

The simplest process for H_2O formation on grain surfaces is the sequential hydrogenation of O atoms:

$$O + H \rightarrow OH, \quad (1)$$

$$OH + H \rightarrow H_2O. \quad (2)$$

Because Reactions (1) and (2) are radical–radical reactions, these reactions have no activation barriers. Hiraoka et al. (1998) examined the above reaction pathways using D atoms instead of H atoms to irradiate O atoms in a N_2O matrix at 12 K, and reported the detection of D_2O by temperature programmed desorption (TPD) spectra through reactions of O atoms with D atoms. However, in their experimental procedures, it is not clear whether D_2O was produced through D addition to O atoms at 12 K or during heating. Subsequent to Reaction (1), H_2O is also produced through the reaction of OH with H_2:

$$OH + H_2 \rightarrow H_2O + H, \quad (3)$$

with an activation barrier of 2600 K (Schiff 1973). Tielens & Hagen (1982) have proposed an alternative route for the formation of H_2O from an oxygen atom:

$$O + O \rightarrow O_2, \quad (4)$$

$$O_2 + H \rightarrow HO_2, \quad (5)$$

$$HO_2 + H \rightarrow H_2O_2, \quad (6)$$

$$H_2O_2 + H \rightarrow H_2O + OH. \quad (7)$$

Reaction (5) has essentially no activation barrier (Walch et al. 1988), and Reaction (7) has an activation energy of approximately 2000 K (Koussa et al. 2006).

Miyauchi et al. (2008) have experimentally demonstrated that H_2O is formed via the addition of H atoms to O_2 at 10 K, where solid O_2 was deposited at 10 K and H or D atoms were then irradiated onto the solid O_2 (hereafter, the experiment is referred to as the H irradiation experiment onto solid O_2). H_2O_2 formation was observed during the experiments, indicating that H_2O is formed through Reactions (5)–(7). In addition, D_2O is also formed through the successive addition of D to solid O_2. They also reported that the ratios of rate constants were $k_1H/k_1D = 1$, while $k_2H/k_2D = 8$, where k_1H and k_2H are the rate constants for H atom addition in Reactions (5) and (7), respectively, and k_1D and k_2D are those for D atom addition, respectively. The former rate constant ratio is consistent with the fact that Reaction (5) has essentially no activation barrier (Walch et al. 1988). The latter result, where the ratio of $k_2H/k_2D = 8$, is reasonably explained as the isotope effect of a tunneling reaction with a reasonable activation energy of ~2000 K (Koussa et al. 2006).

After publication of Miyauchi et al. (2008), Ioppolo et al. (2008) studied the same reactions at 12–28 K. They confirmed our results qualitatively, but not quantitatively. The experiments performed by Ioppolo et al. (2008) were basically similar to those by Miyauchi et al. (2008) except for the type of atomic source, and flux and temperature of H atoms; a thermal-cracking-type H-atom source was used with a nose-shaped quartz pipe to cool down the H atoms to room temperature. The flux of H atoms was not measured, but was estimated to be 5×10^{13} atoms cm^{-2} s^{-1}. Different results for the rate constants of Reactions (5) and (7) were obtained: $k_1H = k_2H$ and $k_1D = k_2D$, which are inconsistent with the barrier height estimations reported by Koussa et al. (2006) and Walch et al. (1988). Furthermore, $k_1H/k_2D = 0.4$ and $k_2H/k_2D = 0.7$ ratios

[1] Author to whom any correspondence should be addressed.

were obtained, which indicate that the reaction of D atoms is faster than that of H atoms. These different results may be due to the method used to determine the reaction rates; different fitting models were used in the initial and latter stages of the reactions, of which the physicochemical meaning is unclear.

In the H irradiation experiment onto solid O_2, the formation of H_2O and H_2O_2 stops at some stage, although some O_2 molecules remain unreacted (Miyauchi et al. 2008; Ioppolo et al. 2008). A similar phenomenon was observed in experiments on the hydrogenation of CO (Watanabe et al. 2004). In order to explain the above observations Miyauchi et al. (2008) proposed a layer model, in which the reaction occurs only at the surface of the deposited O_2, resulting in an onion-like structure of molecular layers with H_2O on the top, H_2O_2 in the middle, and O_2 at the bottom, as suggested by Watanabe et al. (2004). Probably due to the layer structure, abundant H_2O in molecular clouds was not reproduced in the laboratory experiments (Miyauchi et al. 2008; Ioppolo et al. 2008), although the reaction kinetics were revealed by the H irradiation experiments onto solid O_2. In molecular clouds, reactions of H atoms with solid O_2 having a thickness of several monolayers are almost not expected to occur, because O_2 molecules could be continuously formed on the surface through Reaction (4), and then react with H atoms, which eventually results in the formation of H_2O_2 and H_2O on the grain surface (Tielens & Hagen 1982). In order to simulate the reactions in molecular clouds, it is more appropriate that O_2 molecules and H atoms are supplied simultaneously onto a substrate (hereafter, the experiment is referred to as the O_2 and H codeposition experiment), with in situ monitoring of the products. Miyauchi et al. (2008) have demonstrated that Reactions (5)–(7) occur very quickly (<1 minute), even at 10 K, despite the significant activation barrier of Reaction (7) (Koussa et al. 2006). Therefore, it is expected that codeposition of H atoms with O_2 molecules leads to the continuous formation of H_2O_2 and H_2O under conditions closer to those of dense molecular clouds.

In addition to the mechanism for the formation of H_2O, the IR spectral features for H_2O ice in molecular clouds have been of significant interest; the OH-stretching mode of H_2O, the so-called 3 μm band, reflects the structure, composition, and temperature of H_2O-dominated ice (Hagen et al. 1981, 1983). Therefore, the shape of the 3 μm band will be useful for investigating the characteristics of H_2O ice. It has been shown, both observationally (Smith et al. 1989) and theoretically (Kouchi et al. 1994), that the structure of water ice in molecular clouds is amorphous. However, in the H irradiation experiments onto solid O_2, it was very difficult to discuss the structure of H_2O ice, because the shape of the 3 μm band assigned to H_2O was obscured, due to the low levels of product overlapping with H_2O_2 (Miyauchi et al. 2008; Ioppolo et al. 2008). In contrast, it is expected that more H_2O could be formed during continuous codeposition of O_2 with H, which may provide more suitable IR spectral data for examination of the 3 μm band.

In this study, the formation of H_2O from O_2 molecules is re-examined at 10–40 K by the codeposition of O_2 with H atoms onto a substrate. We present new information regarding the temperature dependence of water formation and the structure of amorphous H_2O ice produced by surface reactions, which have not been reported previously. The present study enables us to compare the experimental results with astronomical observations more appropriately than previous experiments.

2. EXPERIMENTAL DETAILS

Experiments were performed using the Apparatus for SUrface Reaction in Astrophysics (ASURA) system. ASURA consists of a main chamber, an atomic source, and a Fourier transform infrared (FTIR) spectrometer. Details of this apparatus have been described previously (Watanabe et al. 2006; Nagaoka et al. 2007). At the center of the main chamber, a mirror-finished aluminum (Al) substrate is mounted on the cold head of a He refrigerator. The base pressure of the main chamber is $\sim 10^{-10}$ torr, but it reaches (1–2) $\times$ 10^{-7} torr during operation of the atomic source. Atomic hydrogen (H) was produced by microwave-induced plasma in a Pyrex tube and transferred via a series of polytetrafluoroethylene (PTFE) and aluminum tubes to the substrate. The atomic beam was cooled to 100 K in the aluminum tube that was connected to another He refrigerator. The flux of H atoms in the present experiment was measured, using the method reported by Hidaka et al. (2007), to be 2 $\times$ 10^{14} atoms cm^{-2} s^{-1}. The O_2 molecules were introduced into the main chamber through a capillary plate located approximately 5 cm from the substrate, with an incident angle of 30° to the normal of the substrate surface. Although O_2 molecules were introduced at room temperature, they were immediately cooled down to the temperature of the substrate once they were absorbed. Because O_2 molecules are IR inactive, the deposition rate of O_2 cannot directly be determined by an IR spectrometer. Instead, for the preparatory experiment, CO molecules were introduced into the main chamber under a condition and the deposition rate of CO was first determined. Then, O_2 molecules were introduced into the chamber under the same deposition (gas flow) condition as that of the CO. Since the conductance of the gas line is considered to be almost the same for O_2 and CO gases, the O_2 deposition rate is nearly equal to that of CO. This assumption is based on the fact that the binding energy of CO on an H_2O surface (1900 K) is very close to that of O_2 (1600 K) (Tielens 2005), and CO and O_2 have a close mass. Deposition rates of O_2 were varied from 7.5 to 380 $\times$ 10^{10} molecules cm^{-2} s^{-1}, which results in O_2/H flux ratios of 3.8 $\times$ 10^{-4} to 1.9 $\times$ 10^{-2}. The O_2/H ratio of 3.8 $\times$ 10^{-4} is the minimum value attainable with this experimental setup, while values larger than 1.9×10^{-2} are possible, but not utilized in this study. The reaction products were monitored in situ by infrared reflection–absorption spectroscopy with a resolution of 4 cm^{-1} through the spectral range of 700–4000 cm^{-1}. The temperature of the Al substrate was maintained at 10–40 K during each experiment. For the experiments with O_2/H ratios of 0.019, 0.009, 0.002, and 3.8 $\times$ 10^{-4}, H and O_2 codeposition was conducted for 90, 120, 360, and 1020 minutes, respectively.

To investigate the effect of amorphous ice on the reactions, similar experiments were performed on a predeposited amorphous D_2O ice with a thickness of $\sim$30 monolayer (ML), where 1 ML indicates the amount of D_2O to form 10^{15} molecules cm^{-2}. Amorphous D_2O ice was produced by vapor deposition at 10 K on the Al substrate with a rate of $\sim$1 ML $minute^{-1}$.

3. RESULTS AND DISCUSSION

3.1. Overview of the Reaction

Under all experimental conditions, both H_2O and H_2O_2 were formed by codeposition of H atoms with O_2 molecules on the Al substrate and amorphous D_2O ice (Figure 1). In the same manner as utilized in the previous experiment (Miyauchi et al. 2008), we confirmed that H_2O and H_2O_2 formed are not contaminants. No

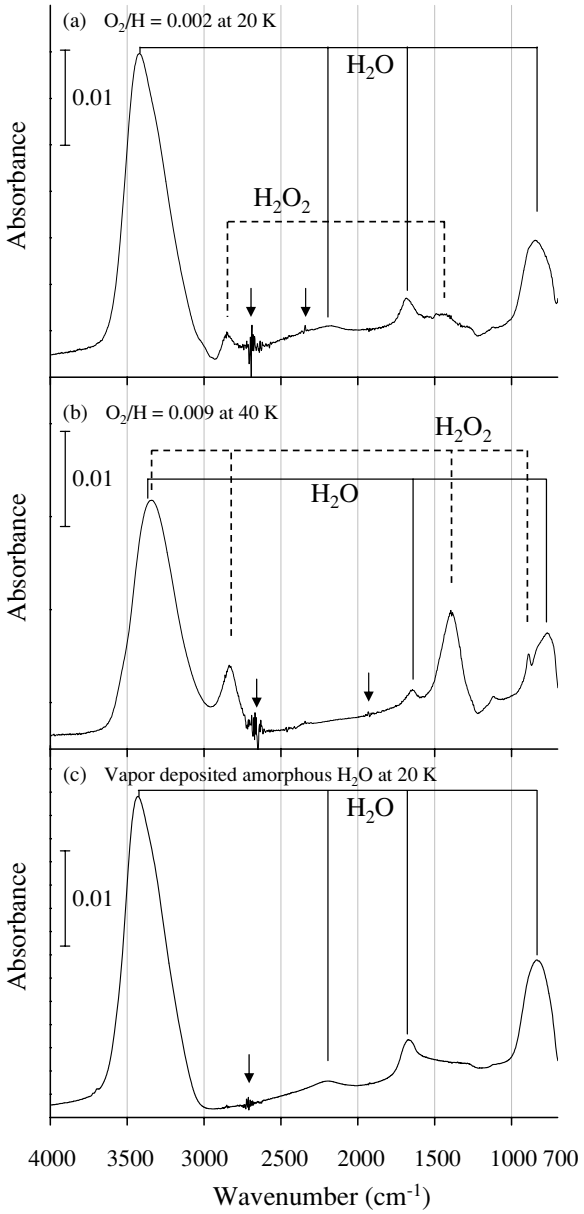

Figure 1. IR spectra of products after codeposition of O_2 with H under conditions of (a) $O_2/H = 0.002$ at 20 K after 360 minutes and (b) $O_2/H = 0.009$ at 40 K after 120 minutes. (c) For comparison, the IR spectra of pure amorphous H_2O ice produced by vapor deposition at 20 K. Solid and dashed lines indicate peaks assigned to H_2O and H_2O_2, respectively. Arrows indicate noise caused by vibration of the He refrigerator.

intermediate radicals such as HO_2 (1142 cm^{-1}, Cooper et al. 2006) were observed in this study, which is consistent with the H irradiation experiment onto solid O_2 (Miyauchi et al. 2008). Ioppolo et al. (2008) showed that, for the H irradiation experiment onto solid O_2, the reactions proceed at temperatures lower than 28 K. This is consistent with O_2 desorption from a Au substrate at temperatures of 29.5–31.3 K in the typical experimental timescale (Acharyya et al. 2007). However, in the codeposition experiments conducted in this study, it is clear that the formation of H_2O and H_2O_2 occurs even at 40 K, which could be above the desorption temperature of O_2.

The reasons for the formation of H_2O and H_2O_2, as observed in the codeposition experiments at temperatures higher than the O_2 desorption temperature, will be discussed. The residence time of a species (τ_r) on a substrate is given by the following equation:

$$\tau_r = \nu_0^{-1} \exp(E_{i-j}/kT), \quad (8)$$

where ν_0 and E_{i-j} are the vibrational frequency and the binding energy of the adsorbed species i on the substrate j, respectively, k is the Boltzmann constant, and T is temperature. The value of E_{O_2-Al} is unknown. Instead, by substituting $E_{O_2-Au} = 912$ K (Acharyya et al. 2007), and ν_0 as 1.4×10^{12} s^{-1} (Tielens 2005), the τ_r of O_2 molecules on the Au substrate are calculated to be ~11 s and 5.7×10^{-3} s at 30 and 40 K, respectively. In contrast, because no data are available for E_{H-Al}, and also for E_{H-Au}, τ_r of H atoms cannot be calculated from equation (8). Then, considering that E_{H-H_2O} (650 K, Al-Halabi & van Dishoeck 2007) is much smaller than $E_{O_2-H_2O}$ (1600 K, Tielens 2005), E_{H-Au} is expected to be much smaller than E_{O_2-Au}, leading to an assumption that τ_r of H atoms is much shorter than that of O_2 molecules on the Au substrate shown above. If these relationships can be applied to the Al substrate, then the results indicate that Reactions (5)–(7) proceed quickly enough, so that H_2O and H_2O_2 are produced within the short residence time of H and O_2 before the H atoms and O_2 molecules desorb from the Al substrate. Once H_2O and H_2O_2 are formed, these products can remain even at 40 K because of their high desorption temperatures.

3.2. Formation of Compact Amorphous Ice

Figures 1(a) and (b) show examples of IR spectra after codeposition of H with O_2 obtained with an O_2/H ratio of 0.002 at 20 K and with an O_2/H ratio of 0.009 at 40 K, respectively. For comparison, Figure 1(c) shows an IR spectrum of the amorphous H_2O ice produced by vapor deposition at 20 K with a rate of ~0.4 ML $minute^{-1}$. Some peaks in Figure 1 are assigned to H_2O (3414, 2173, 1683, and 843 cm^{-1}) and H_2O_2 (3340, 2837, 1394, and 888 cm^{-1}). The OH-stretching mode (3414 cm^{-1}) in Figure 1(a) is almost the same as that for the vapor-deposited amorphous H_2O ice (Figure 1(c)), which indicates that the H_2O ice formed in this experiment is amorphous (Bergren et al. 1978; Hagen et al. 1981). The spectral feature is consistent with the observations of H_2O ice in molecular clouds (e.g., Hagen et al. 1981; van de Bult et al. 1985; Smith et al. 1989) and theoretical studies (Kouchi et al. 1994). However, the width of the 3 μm band of ice produced after the codeposition is slightly wider in the small-wavenumber region than that of vapor-deposited amorphous H_2O ice at 20 K (Figure 2). Hagen et al. (1981) showed that the width of the 3 μm band becomes irreversibly narrower with temperature; however, the results of the present study do not exhibit such a tendency. It is therefore concluded that the wider 3 μm band from the codeposition experiment is not due to local heating by the heat of reactions, but is probably due to the overlapping of the H_2O_2 band. Although the heats of reaction (2.1, 3.7, and 3.9 eV for Reactions (5), (6), and (7), respectively;[2] 4.5 eV for H–H recombination) are considerably large, it is suggested that the heats of reactions do not affect the microscopic structure of amorphous H_2O ice. This suggestion is consistent with the theoretical discussion by Kouchi et al. (1994).

Two small peaks assigned to the dangling OH bonds are typically observed in the spectrum for vapor-deposited amorphous H_2O ice at 3721 and 3698 cm^{-1} (Figure 3(a)), and these are assigned to two- and three-coordinated surface H_2O molecules,

[2] NIST CCCBDB Web site; http://cccbdb.nist.gov/hf0k.asp.

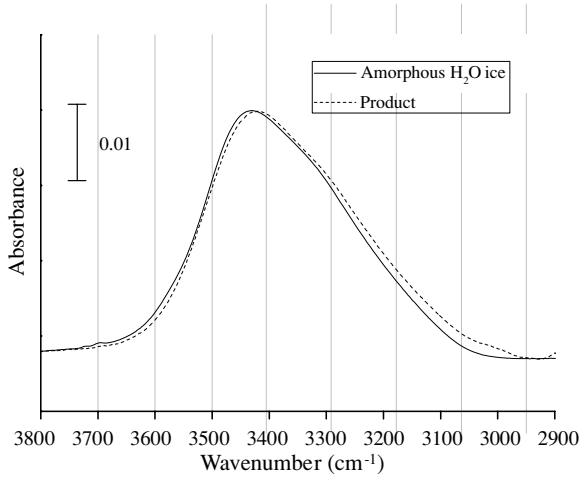

Figure 2. Comparison of IR spectra designated as the OH-stretching mode for the product of O_2–H codeposition and pure amorphous H_2O ice produced by vapor deposition at 20 K.

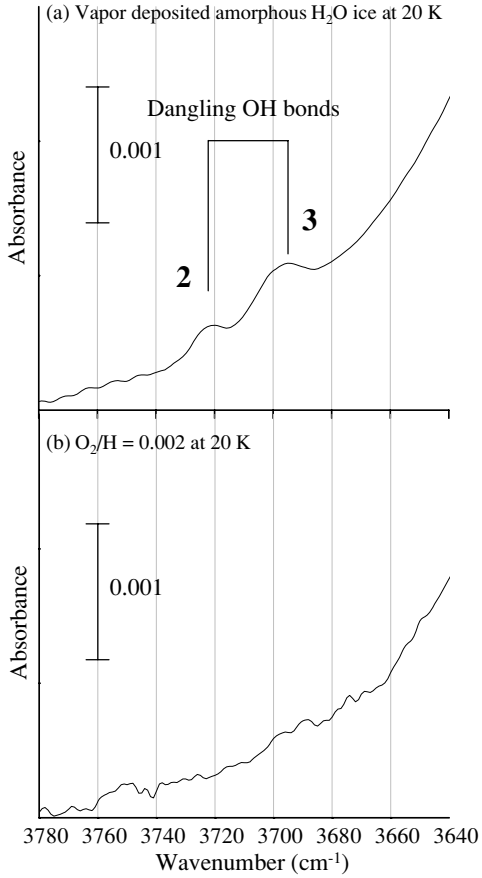

Figure 3. IR spectra of (a) pure amorphous H_2O ice produced by vapor deposition at 20 K and (b) products of the codeposition experiments under the conditions of $O_2/H = 0.002$ at 20 K. Peaks numbered with 2 and 3 in (a) indicate two- and three-coordinated dangling OH bonds, respectively.

respectively (Buch & Devlin 1991). However, these peaks are not observed in the amorphous H_2O ice formed by codeposition (Figure 3(b)). The dangling OH bonds appear in the IR spectrum for amorphous H_2O ice due to the microporous structure (Buch & Devlin 1991; Rowland & Devlin 1991; Zondlo et al. 1997). On the other hand, it has been reported that the dangling OH bonds disappear when the amorphous ice is annealed to 120 K (Rowland & Devlin 1991; Zondlo et al. 1997), when the ice is irradiated with 200 keV protons at 15 K (Palumbo 2006), or when the ice is irradiated with 100 keV Ar^+ ions at 40 K (Raut et al. 2007), all of which are due to collapse of the microporous structure. Although the peak position of the dangling OH bonds of H_2O_2–H_2O mixed ice (3664 cm^{-1}, Palumbo 2006) is different from that of vapor-deposited pure amorphous H_2O ice (3698 and 3721 cm^{-1}), such a feature does not appear in the IR spectrum of amorphous H_2O ice formed by codeposition (Figure 3(b)). The lack of dangling OH bonds in H_2O ice formed by codeposition is consistent with the feature for H_2O ice in molecular clouds (Keane et al. 2001). It was confirmed that codeposition of O_2 and H_2O molecules at various ratios also produces spectral bands for dangling bonds, which indicates that the bands do not disappear due to the coexistence of O_2 and H_2O. Therefore, the less clear signature of dangling OH bonds in Figure 3(b) implies that the structure of the amorphous H_2O ice formed by codeposition is more compact compared with vapor-deposited amorphous H_2O ice. This might be due to the heats of reactions. Small amounts of H_2O_2 present with H_2O may also contribute to the lack of dangling OH bonds.

3.3. Conditions for Abundant H_2O Formation

It is known that the peak positions assigned to the OH-stretching mode for both H_2O and H_2O_2 molecules (3000–3600 cm^{-1}) overlap with each other in the IR spectrum of H_2O–H_2O_2 mixed ice (Boudin et al. 1998); therefore, the peak is not suitable for quantification. Instead, the peaks assigned to the OH-bending mode for H_2O (1590–1740 cm^{-1}) and H_2O_2 (1270–1530 cm^{-1}) were used to obtain their abundances in this study. The column densities are calculated from our obtained peak areas and the previously reported integrated band strengths, as described in Hidaka et al. (2007) in which correction for the light path with an IR incident angle of about 83° was made. The band strengths used are 1.2×10^{-17} and 2.1×10^{-17} cm $molecules^{-1}$ for H_2O and H_2O_2, respectively, which are obtained by the *transmission* absorption spectroscopy of pure amorphous H_2O ice (Gerakins et al. 1995) and the *reflection* absorption spectroscopy of H_2O_2 in solid mixture (Loeffler et al. 2006), respectively. Our estimates of column densities by the reflection absorption spectroscopy can include some errors especially in H_2O due to the use of band strength obtained by the transmission spectroscopy. In order to check the difference in column density estimates between the transmission and reflection methods, we also performed the transmission spectroscopy for pure amorphous H_2O ice and pure solid CO and found that using the same reported band strength the difference in the estimated column densities between the transmission and reflection methods is within approximately a factor of 2. It should be noted that even in the transmission spectroscopy, it is very difficult to derive the exact column densities of molecules in solid mixture. Furthermore, all of our discussion in the present study is based on the relative column densities. Therefore, we conclude that our estimated column densities are reasonably acceptable.

Figure 4 presents typical variations in the column densities of H_2O and H_2O_2 as a function of time. These molecules display a linear increase, because the source materials (O_2 + H) that can yield H_2O_2 and H_2O are continuously supplied. The results clearly show that the relative abundance of H_2O and H_2O_2 (H_2O/H_2O_2) varies with the experimental conditions. For example, under conditions with an O_2/H ratio of 0.002 at 20 K (Figure 4(a)), the H_2O/H_2O_2 ratio is approximately 5.

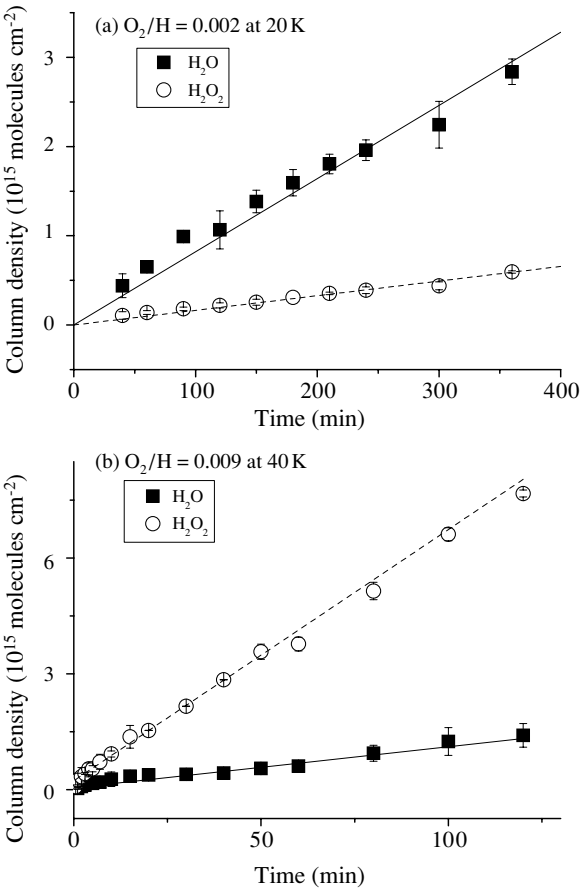

Figure 4. Variations in the column density of H_2O and H_2O_2 after codeposition of O_2 with H under the conditions of (a) O_2/H = 0.002 at 20 K and (b) O_2/H = 0.009 at 40 K.

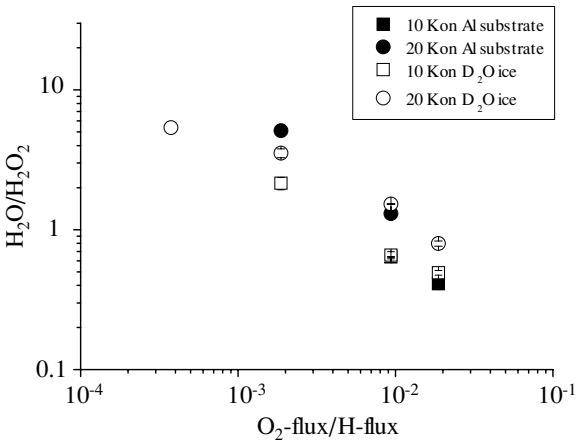

Figure 5. H_2O/H_2O_2 ratio vs. O_2/H at 10 and 20 K. Open and solid symbols represent the experimental results for codeposition with and without amorphous D_2O ice, respectively.

However, under conditions with an O_2/H ratio of 0.009 at 40 K (Figure 4(b)), the H_2O/H_2O_2 ratio is approximately 0.15. Figure 5 shows that as the O_2/H flux ratio decreases, the H_2O/H_2O_2 ratio increases up to approximately 5, which is qualitatively understandable when considering the onion-like structure described in section 1. When the O_2 flux is large, O_2 molecules on the surface, as well as H_2O_2 formed by Reaction (6), are covered with additional O_2 prior to subsequent Reaction (7) that produces H_2O. Since the H atoms cannot react with molecules buried in the bulk, part of the buried O_2 and H_2O_2 remains unreacted. Therefore, when the O_2 flux is large, most H atoms are used for the reaction with O_2 rather than H_2O_2, which leads to ice with a smaller H_2O/H_2O_2 ratio. On the other hand, when the O_2 flux is small, O_2 and H_2O_2 have more opportunity to react with H atoms to form H_2O before being covered by additional O_2, which leads to ice with a larger H_2O/H_2O_2 ratio. However, it is interesting to note that although the H flux is quantitatively 2–4 orders of magnitude larger than the O_2 flux, the H_2O/H_2O_2 ratio is still sensitive to the change in the O_2/H ratio. In the gas phase, when the number density ratio of two reactant partners is significant, the final yields exhibit little dependence on the ratio. That is, reactions will eventually proceed to completion until the reactants are consumed.

The present results are readily understandable when the following factors are considered. In the present case, comparison of the sum of column densities of products with H atom fluence shows that, at most, only ∼2% of H atoms are used for the hydrogenation of O_2. This is consistent with a previous study in which only a small portion of H atoms (∼0.1%) was consumed for hydrogenation of CO (Watanabe et al. 2004). Therefore, most of the H atoms are used for the formation of H_2 by recombination. Recombination is a no-barrier radical–radical reaction and has a rate proportional to the square of the H atom density at the surface. Therefore, under the condition of a very high H-atom flux, recombination proceeds preferentially compared with the hydrogenation of O_2. As a result, the number of H atoms used for hydrogenation reactions in the present experiment is much smaller than that irradiated onto the substrate.

At an O_2/H ratio of ∼0.009, the H_2O/H_2O_2 ratio varies with temperature (Figure 6); at 10 K, the H_2O/H_2O_2 ratio is approximately 0.6, while it becomes approximately 1.3 at 20 K. At 30 and 40 K, the H_2O/H_2O_2 ratio is significantly smaller than that at 10 and 20 K, both at approximately 0.15. The temperature dependence of H_2O/H_2O_2 is related to the residence time and the H-atom surface diffusion distance. At 10 K, both H and O_2 can reside on the surface for sufficient time to react by a tunneling process (Miyauchi et al. 2008). At 20 K, the H atoms are assumed to be more mobile on the surface than at 10 K; therefore, more H atoms can meet and react with O_2 and H_2O_2 which results in the formation of more H_2O. On the other hand, at 30 and 40 K, the tunneling Reaction (7) becomes less effective, due to the very short residence time of H atoms on the surface. However, the formation of H_2O_2 occurs regardless of the very short residence times of O_2 and H because Reaction (5) has essentially no barrier (Walch et al. 1988). These characteristics result in smaller values of H_2O/H_2O_2 (Figure 4).

In addition to reactions that produce H_2O_2 and H_2O, the following H-subtraction reactions,

$$HO_2 + H \rightarrow O_2 + H_2, \quad (9)$$

$$H_2O_2 + H \rightarrow HO_2 + H_2, \quad (10)$$

$$H_2O + H \rightarrow OH + H_2, \quad (11)$$

must be considered to discuss the H_2O/H_2O_2 ratio of the products. Reaction (11) is an endothermic reaction (Brouard et al. 2002); therefore, H subtraction from H_2O can be neglected under the present experimental conditions. As for Reactions (9) and (10) on the surface, no data are available for the activation

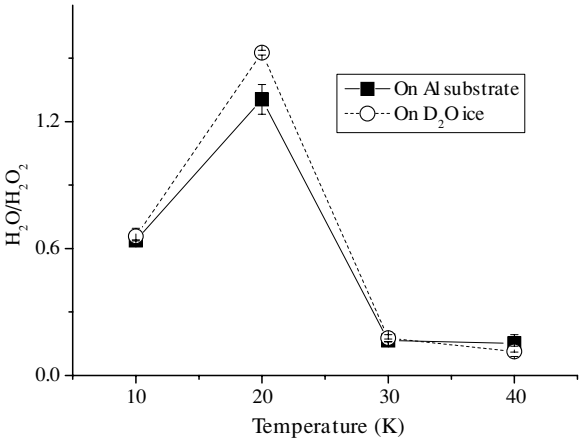

Figure 6. H_2O/H_2O_2 ratio vs. temperature under constant O_2/H (0.009) conditions. Open and solid symbols represent the experimental results for codeposition with and without amorphous D_2O ice, respectively.

energy. In the gas phase, it is reported that the barrier heights for Reactions (9) and (10) are 1070 K (Lee & Hochgreb 1998) and 1890–4780 K (Lee & Hochgreb 1998; Tarchouna et al. 2006), respectively. Despite the relatively low barrier height for Reaction (9), the progress of the reaction should be negligible, because Reaction (5) proceeds with essentially no barrier (Walch et al. 1988) and Reaction (6) proceeds much faster than Reaction (5) (Miyauchi et al. 2008). The barrier height of Reaction (10) is almost the same or slightly higher than that for Reaction (7) (∼2000 K, Koussa et al. 2006), which suggests that H_2O_2 formed by Reaction (6) could be used for both Reactions (7) and (10). However, the high H_2O/H_2O_2 ratio of 5 obtained for a small O_2/H flux ratio of 0.002 demonstrates that even if H subtraction from H_2O_2 proceeds to some extent, Reaction (10) would have little contribution to the H_2O/H_2O_2 ratio of the products, because the product of Reaction (10), HO_2, is quickly hydrogenated again by additional H atoms to yield H_2O_2 by Reaction (6).

The hydrogenation of O_2 to form H_2O proceeds even at 40 K in the codeposition experiments, regardless of the presence of amorphous D_2O ice as the substrate. The variations in H_2O/H_2O_2 with temperature, both with and without amorphous D_2O ice, are quite similar (Figure 6). However, previous studies reported that amorphous ice has a catalytic effect to enhance the reaction rate for reactions of H atoms with CO molecules (e.g., Hidaka et al. 2007) and H–D substitution of solid methanol (Watanabe & Kouchi 2008). In addition, it has been theoretically demonstrated that H_2O molecules have a catalytic effect to reduce the reaction barrier height of some surface reactions (Woon 2002; Xie et al. 2006). Although such a catalytic effect is not clearly observed for the value of H_2O/H_2O_2 in the present study, we suggest that the effect could occur in the formation of H_2O and H_2O_2 from O_2. This is because when H atoms are irradiated onto 30 ML amorphous D_2O ice covered with 3 ML O_2, H_2O and H_2O_2 are formed even at 40 K, while the formation of these molecules is not observed above 23 K without amorphous ice (Y. Oba et al. 2009, in preparation).

4. ASTROPHYSICAL IMPLICATIONS

It is widely recognized that H_2O ice in dense molecular clouds is amorphous (e.g., Smith et al. 1989). Amorphous H_2O ice produced by vapor deposition in the laboratory contains micropores (Mayer & Pletzer 1986), and these pores contain dangling OH bonds. Therefore, it has been implied that amorphous ice in dense molecular clouds may have a large number of dangling bonds. However, there have been no reports on the detection of dangling bonds in interstellar ices (Keane et al. 2001). To explain this, two possibilities have been suggested: (1) there are no significant amounts of micropores formed with the formation of amorphous H_2O ice; (2) dangling bonds are present at the formation of amorphous H_2O ice, but disappear due to cosmic ray irradiation (Palumbo 2006; Raut et al. 2007). However, the former possibility has not been experimentally investigated. The present study clearly demonstrates that amorphous H_2O ice does not exhibit bands for dangling bonds when it is formed by surface atomic reactions.

In addition to the lack of dangling OH bonds, the IR spectra of amorphous H_2O ices in molecular clouds have a characteristic feature at 3.2–3.5 μm, which is referred to as the long-wavelength wing (Smith et al. 1989) or low-frequency wing (Hagen et al. 1983). It has been considered that the wing is derived from the absorption of ammonia (Merrill et al. 1976), hydrated silicates (Knacke & Krätschmer 1980), hydrocarbons (Smith et al. 1989), or methanol (Grim et al. 1991). The contributions from ammonia and hydrous silicates to the wing were ruled out by Smith et al. (1989). However, the source of the long-wavelength wing is still unclear to date. In addition to these candidate species, another candidate is proposed from the present study, in that small amounts of H_2O_2 may explain the long-wavelength wing, as shown in Figure 2. Although the presence of H_2O_2 in molecular clouds has not been confirmed (see below), the weak absorption at 2900–3300 cm^{-1} (Figure 2) is similar to previously reported astronomical observations (e.g., Smith et al. 1989).

In contrast to the ubiquitous presence of water, hydrogen peroxide has not been observed in molecular clouds. Blake et al. (1987) theoretically estimated that the H_2O/H_2O_2 ratio is approximately 30 in the core of the Orion molecular cloud. In addition, the upper limit of H_2O_2 abundances in the NGC7538:IRS9 protostar has been estimated to be <0.5 compared to H_2O abundances (Boudin et al. 1998). The H_2O/H_2O_2 ratio in these environments is considerably high when compared to that obtained in the present study (up to ∼5). If the O_2/H ratio is extrapolated to a lower value ($\sim 1 \times 10^{-4}$), then the expected H_2O/H_2O_2 ratio becomes 15 to 30 (Figure 5). However, in molecular clouds, O_2 is formed by the reaction of two oxygen atoms (Reaction (4)) absorbed on a grain surface, followed by reactions with H atoms to produce H_2O_2 and H_2O (Reactions (5)–(7)). Furthermore, there remains some uncertainty regarding the absolute abundance of O and H atoms in molecular clouds. Therefore, an O_2/H ratio of $\sim 1 \times 10^{-4}$ with an estimated abundance of H_2O/H_2O_2 (15 to 30) may not correspond directly with the actual H_2O/H_2O_2 ratio in molecular clouds. The probability of H–H recombination is proportional to the square of the number of H atoms on a surface (Vidali et al. 2007); therefore, the fraction of H atoms consumed by recombination becomes smaller, and that consumed by hydrogenation of O_2 becomes larger under the condition of low H flux in molecular clouds. Thus, in molecular clouds, the ratio of H_2O/H_2O_2 tends to be larger than that in the present experiments. Regardless, the experimental results cannot be applied directly for discussion of the actual H_2O/H_2O_2 versus O/H ratios in molecular clouds at present. For future work, the kinetics of Reactions (2) and (3) and astronomical observations of H_2O_2 are required for the further elucidation of H_2O formation mechanisms and the relative abundance of H_2O_2.

This work was partly supported by a Grand-in-Aid for Scientific Research from the Japan Society for the Promotion of Science.

REFERENCES

Acharyya, K., Fuchs, G. W., Fraser, H. J., van Dishoeck, E. F., & Linnartz, H. 2007, A&A, 466, 1005
Al-Halabi, A., & van Dishoeck, E. F. 2007, MNRAS, 382, 1648
Bergren, M. S., Schuh, D., Sceats, M. G., & Rice, S. A. J. 1978, J. Chem. Phys., 68, 3477
Blake, G. A., Sutton, E. C., Masson, C. R., & Phillips, T. G. 1987, ApJ, 315, 621
Boudin, N., Schutte, W. A., & Greenberg, J. M. 1998, A&A, 331, 749
Brouard, M., O'Keeffe, P., & Vallance, C. 2002, J. Phys. Chem. A, 106, 3629
Buch, V., & Devlin, J. P. 1991, J. Chem. Phys., 94, 4091
Cooper, P. D., Moore, M. H., & Hudson, R. L. 2006, J. Phys. Chem. A, 110, 7985
Cuppen, H. M., & Herbst, E. 2007, ApJ, 668, 294
d'Hendecourt, L. B., Allamandola, L. J., & Greenberg, J. M. 1985, A&A, 152, 130
Gerakins, P. A., Schutte, W. A., Greenberg, J. M., & van Dishoeck, E. F. 1995, A&A, 296, 810
Gibb, E. L., Whittet, D. C. B., Boogert, A. C. A., & Tielens, A. G.. G. M. 2004, ApJS, 151, 35
Grim, R. J. A., Baas, F., Geballe, T. R., Greenberg, J. M., & Schutte, W. 1991, A&A, 243, 473
Hagen, W., Tielens, A. G. G. M., & Greenberg, J. M. 1981, Chem. Phys., 56, 367
Hagen, W., Tielens, A. G. G. M., & Greenberg, J. M. 1983, A&A, 117, 132
Hasegawa, T. I., & Herbst, E. 1993, MNRAS, 261, 83
Hasegawa, T. I., Herbst, E., & Leung, C. M. 1992, ApJS, 82, 167
Hidaka, H., Kouchi, A., & Watanabe, N. 2007, J. Chem. Phys., 126, 204707
Hiraoka, K., Miyagoshi, T., Takayama, T., Yamamoto, K., & Kihara, Y. 1998, ApJ, 498, 710
Ioppolo, S., Cuppen, H. M., Romanzin, C., van Dishoeck, E. F., & Linnartz, H. 2008, ApJ, 686, 1474
Keane, J. V., Boogert, A. C. A., Tielens, A. G. G. M., Ehrenfreund, P., & Schtte, W. A. 2001, A&A, 375, L43
Knacke, R. F., & Krätschmer, W. 1980, A&A, 92, 281
Kouchi, A., Yamamoto, T., Kozasa, T., Kuroda, T., & Greenberg, J. M. 1994, A&A, 290, 1009
Koussa, H., Bahri, M., Jaïdane, N., & Ben Lakhdar, Z. 2006, J. Mol. Struct., 770, 149
Lee, D., & Hochgreb, S. 1998, Int. J. Chem. Kinetics, 30, 385
Loeffler, M. L., Teolis, B. D., & Baragiola, R. A. 2006, J. Chem. Phys., 124, 104702
Mayer, E., & Pletzer, R. 1986, Nature, 319, 298
Merrill, K. M., Russell, R. W., & Soifer, B. T. 1976, ApJ, 207, 763
Miyauchi, N., Hidaka, H., Chigai, T., Nagaoka, A., Watanabe, N., & Kouchi, A. 2008, Chem. Phys. Lett., 456, 27
Nagaoka, A., Watanabe, N., & Kouchi, A. 2007, J. Phys. Chem. A, 111, 3016
Palumbo, M. E. 2006, A&A, 453, 903
Raut, U., Teolis, B. D., Loeffler, M. J., Vidal, R. A., Famá, M., & Baragiola, R. A. 2007, J. Chem. Phys., 126, 244511
Rowland, B., & Devlin, J. P. 1991, J. Chem. Phys., 94, 812
Schiff, H. I. 1973, Physics and Chemistry of Upper Atmospheres (Dordrecht: Reidel)
Smith, R. G., Sellgren, K., & Tokunaga, A. T. 1989, ApJ, 344, 413
Tarchouna, Y., Bahri, M., Jaïdane, N., & Lakhdar, Z. B. 2006, J. Mol. Struct., 758, 53
Tielens, A. G. G. M. 2005, The Physics and Chemistry of the Interstellar Medium (Cambridge: Cambridge Univ. Press)
Tielens, A. G. G. M., & Hagen, W. 1982, A&A, 114, 245
van de Bult, C. E. P. M., Greenberg, J. M., & Whittet, D. C. B. 1985, MNRAS, 214, 289
Vidali, G., et al. 2007, J. Phys. Chem. A, 111, 12611
Walch, S. P., Rohlfing, C. M., Melius, C. F., & Baushlicher, C. W. 1988, J. Chem. Phys., 88, 6273
Watanabe, N., & Kouchi, A. 2008, Prog. Surf. Sci., 83, 439
Watanabe, N., Nagaoka, A., Hidaka, H., Shiraki, T., Chigai, T., & Kouchi, A. 2006, Planet. Space Sci., 54, 1107
Watanabe, N., Nagaoka, A., Shiraki, T., & Kouchi, A. 2004, ApJ, 616, 638
Woon, D. E. 2002, ApJ, 569, 541
Xie, H.-B., Ding, Y.-H., & Sun, C.-C. 2006, ApJ, 643, 573
Zondlo, M. A., Onasch, T. B., Warshawsky, M. S., Tolbert, M. A., Mallick, G., Arentz, P., & Robinson, M. S. 1997, J. Phys. Chem. B, 101, 10887